Stochastic Simulation of Utility-Scale Storage Resources in Power Systems With Integrated Renewable Resources

Yannick Degeilh and George Gross, *Fellow, IEEE*

***Abstract*—We report on the extension of a general stochastic simulation approach for power systems with integrated renewable resources to also incorporate the representation of utility-scale storage resources. The extended approach deploys models of the energy storage resources to emulate their scheduling and operations in the transmission-constrained hourly day-ahead markets. To this end, we formulate a scheduling optimization problem to determine the operational schedule of the controllable storage resources in coordination with the demands and the various supply resources, including the conventional and renewable resources. The incorporation of the scheduling optimization problem into the Monte Carlo simulation framework takes full advantage of the structural characteristics in the construction of the so-called sample paths for the stochastic simulation approach and to ensure its numerical tractability. The extended methodology has the capability to quantify the power system economics, emissions and reliability variable effects over longer-term periods for power systems with the storage resources. Applications of the approach include planning and investment studies and the formulation and analysis of policy. We illustrate the capabilities and effectiveness of the simulation approach on representative study cases on modified *IEEE* 118 and *WECC* 240-bus systems. These results provide valuable insights into the impacts of energy storage resources on the performance of power systems with integrated wind resources.**

***Index Terms*—Discrete random processes, emissions, energy storage resources, Monte Carlo/stochastic simulation, production costing, reliability, renewable resource integration, sample paths, transmission-constrained day-ahead markets.**

I. Introduction

STORAGE devices offer substantial benefits to system operations by providing the flexibility to mitigate the effects of variable renewable energy sources and the ability to supply energy and capacity-based ancillary services [1]–[4]. Effective storage deployment can, moreover, obviate or defer the need for specific transmission improvements and/or addition of new generation resources. The ability to exploit the increased flexibility imparted by storage applications to the power system hinges on the development of appropriate models, methodologies and tools, and the formulation of effective policy initiatives. A particularly acute need is a practical simulation tool that can emulate, with good fidelity, the expected variable effects in transmission-constrained systems with integrated renewable and utility-scale energy storage resources (*ESR*s).

We report on the extension of a Monte Carlo simulation approach [5] to represent the impacts on the hourly transmission-constrained day-ahead market (*DAM*) outcomes of the operations of multiple integrated *ESR*s interacting with the demands and renewable/conventional resource outputs. We consider *MWweek*-scale *ESR*s that are, typically, scheduled over horizons ranging from a few days to a week. Examples of such utility-scale *ESR*s include pumped-hydro storage, compressed-air energy storage (*CAES*) and some types of battery technologies, such as sodium sulfur (*NaS*) and flow batteries [1, p. 39]. Moreover, we assume that the *ESR*s are deployed as a system resource by the Independent System Operator (*ISO*). In such a context, the *ESR* outputs are not offered into the market, as is the case for speculative sellers; rather, the *ESR*s are *ISO*-controlled and operated in such a way as to bring maximum economic benefits to the side-by-side power system and *DAM* operations over the specified time period. To this end, the *DAM* clearing mechanism must be adapted to recognize and exploit arbitrage opportunities in the operations of *ESR* in coordination with the clearing of the demands and conventional/renewable resource outputs. By contrast, *ESR*s that are operated for-profit by a speculative seller have their outputs offered into the *DAM*s. In such a case, the scheduling of the *ESR* is the responsibility of the speculative seller, who specifies the offer quantity and price (bid quantity and willingness-to-pay, when it comes to purchasing energy from the market to charge the storage resource) of the *ESR* with the objective to maximize his own profit over the specified time-period. We point out that, once the offering/bidding strategy of the speculative seller is known, for-profit *ESR* participation in the *DAM* is represented by its offer quantity and price (bid quantity and willingness-to-pay), similarly to that of a conventional generation resource (load). Therefore, our approach is in contrast to the large body of literature that investigates the operations and impacts of hybrid wind-storage systems [6]–[9] and the participation of *ESR*s in the markets

Manuscript received February 03, 2014; revised May 07, 2014, June 11, 2014, and June 22, 2014; accepted June 23, 2014. This work was supported in part by the U.S. Department of Energy through "The Future Grid to Enable Sustainable Energy Systems", an initiative of the Power Systems Engineering Research Center (PSERC), the Stanford University Global Climate and Energy Project (GCEP) and the PSERC funding for the Project S-40 "Integration of Storage Devices into Power Systems with Renewable Energy Sources". Paper no. TPWRS-00161-2014.

The authors are with the Department of Electrical and Computer Engineering, University of Illinois at Urbana-Champaign, Urbana, IL 61821 USA (e-mail: degeilh1@illinois.edu; gross@illinois.edu).

Color versions of one or more of the figures in this paper are available online at http://ieeexplore.ieee.org.

Digital Object Identifier 10.1109/TPWRS.2014.2339226

as for-profit, independent resources [10]–[13]. Our work falls in a different thread of research, that for which the *ESR*s are assumed to be controlled by a central entity—the *ISO* for example. Most papers in that area primarily seek to develop optimal strategies for storage resource operations in the short run, with an evident operational planning perspective [14]–[17]. The stochastic programming frameworks used in these works, while very well detailed, require extensive computations and as such, do not lend themselves to the simulation of power system with integrated renewable and storage resources over extended periods of time. Our approach adopts a longer-term planning perspective and is developed with the objective to evaluate the impacts on the variable effects of *MWweek*-scale *ESR*s deployed as *system resources*[1] in power systems with integrated renewable resources. More specifically, the deployment of the proposed extended stochastic simulation approach is to assess, over longer duration periods, the *ESR* impacts on power grid variable effects in terms of economics, reliability and emissions. The paper explicitly considers *ESRs* and their interactions with the other resources, including the variable renewable resources and time-varying demand. Moreover, the various sources of uncertainty under which the power systems operate in the competitive electricity market environment with full consideration of grid constraints, are explicitly represented.

The extended stochastic simulation approach retains the infrastructure and the core aspects of the methodology in [5] and incorporates the steps to appropriately represent the *ESR* operations, which strongly depend on the loads and the outputs of the conventional and renewable resources. Specifically, we retain the representation of the demands and supply-resources with discrete-time random processes (*r.p.s*). Such models account for not only the uncertain and time-dependent behavior of the demands/resource outputs, but also the spatial correlations among the various load/resource sites as well as their temporal correlations. Our simulation methodology uses systematic sampling mechanisms based on Monte Carlo simulation techniques to generate the realizations—the so-called sample paths (*s.p.s*)—of the various *r.p.s* that represent the sources of uncertainty in the demands/resource outputs [5]. Based on such *s.p.s*, we determine the offers and demands to be used as inputs into the hourly *DAM*s in a simulation period of one-week duration. The incorporation of *ESR*s requires that we schedule their operations over multiple time periods so as to adequately represent their charge/discharge cycles. Such a requirement entails modifications in the Monte Carlo simulation methodology in [5] which emulates the solution to a sequence of 168 *separate OPFs* to represent the clearing of the 168 hourly *DAM*s in a weekly simulation period, as part of a so-called *simulation run*. In this work, we construct the so-called *scheduling optimization problem* (*SOP*) and deploy it as the basic mechanism in the extension of the stochastic simulation framework in [5] to represent the impacts of *ESR*s on the *DAM* outcomes over a week-long period. We formulate the *SOP* as a multi-period optimization able to take advantage of arbitrage opportunities in the operations of each *ESR* so as to meet the demand together with the set of conventional and renewable resources, and with the intertemporal *ESR* operational constraints fully considered. Conceptually, absent the representation of the *ESR*s and their operational intertemporal constraints, the *SOP*, defined over the 168 periods of a weekly simulation period, solves the identical problem as that solved by the 168 separate *OPF*s that clear the hourly *DAM*s in [5]. As such, the *SOP* formulation is used to emulate both the *DAM* outcomes and the *ESR* schedules over the weekly simulation period. In the extended simulation framework, we use the *SOP* to map the *s.p.s* of the input *r.p.s*—the demands, renewable resource outputs at various sites and the conventional generation available capacities—into the *s.p.s* of the market outcome *r.p.s*, including the *ESR* operations, locational marginal prices (*LMP*s), congestion rents, supply-side revenues, wholesale purchase payments and the emissions, as well as the contributions to the *LOLP* and *EUE* indices. The market outcomes serve to compute the performance metrics of interest, analogously to the scheme presented in [5]. In fact, in this manner we also obtain the hourly expected stored energy of each *ESR* and the associated discharge output/load charge load over the week-long simulation period.

The extended methodology is therefore able to evaluate the impacts of storage integration into a grid with renewable resources, taking explicitly into account various sources of uncertainty, renewable variability and intermittency and the impacts of the transmission constraints on the deliverability of the electricity to the loads. The effective deployment of the *SOP* is critical in the quantification of the variable effects of large-scale power systems with storage and variable renewable resources operating in a market environment in terms of economics, reliability and emissions. There is a broad range of applications of the simulation methodology to planning, investment, transmission utilization and policy formulation and analysis studies for systems with integrated storage and variable energy sources. In addition, the methodology is very useful in the quantitative study of a broad array of *what if* questions.

The remainder of the paper consists of three sections. In Section II, we discuss the modeling of the *ESR*s and state the mathematical formulation of the *SOP*. In Section III, we briefly summarize the salient aspects of the approach in [5] and describe the steps taken in its extension to incorporate the representation of the *ESR*s. We also provide some details on the implementational aspects of the extended simulation approach. In Section IV, we illustrate the capabilities of the methodology with representative case studies that focus on the economic, reliability and environmental impacts of *ESR* in systems with integrated wind resources. We also present a case study on the economic impacts of *ESR* siting. We conclude in Section V with a summary.

II. *ESR* Modeling and *SOP* Formulation

We devote this section to describe the modeling of the utility-scale *ESR*s and the formulation of the mathematical statement of the *SOP* that is solved to determine the hourly *ESR* operations. We discretize the time axis so as to adopt the granularity used in most North American *DAM*s, i.e., we adopt an hour as the shortest indecomposable period of time. As such, all the variables/parameters in the *ESR* models are indexed by the hour,

[1]We note that our approach is still able to represent the impacts of for-profit *ESR*s, so long as the offering strategies of the associated speculative sellers are known.

and the *ESR* operations are scheduled on an hourly basis. We denote by $x[h]$ the variable x in hour h and use the notation given in the Appendix.

A. Modeling of the ESRs

We consider the set $\mathcal{E} = \{e : e = 1, \ldots, E\}$ of *ESR*s. Each *ESR* $e \in \mathcal{E}$ acts either as a load in hours during which it charges, or as a generation resource in hours during which it discharges. In other hours, it remains idle with no impact on the side-by-side power system and market operations. We assume that the operational state—discharge, charge or idle—of *ESR* e, together with its associated *MW* discharge output $g^e[h]$ (charging load $\ell^e[h]$), remain unchanged over the duration of a particular hour h. We introduce the binary variables $u_g^e[h]$, $u_\ell^e[h] \in \{0, 1\}$ to specify the operational state of *ESR* e in hour h. Binary variable $u_g^e[h]$ ($u_\ell^e[h]$) takes value 1 if *ESR* e discharges (charges) during hour h, 0 otherwise. We enforce the physical fact that an *ESR* cannot both charge and discharge at the same time, that is, $u_g^e[h]$ and $u_\ell^e[h]$ cannot be both equal to 1, by requiring that for each hour h, $u_g^e[h] + u_\ell^e[h] \leq 1$. *ESR* e is said to be idle when it neither discharges nor charges, i.e., $u_g^e[h] = u_\ell^e[h] = 0$. We also denote by $(\kappa_g^e)^M$ ($(\kappa_\ell^e)^M$) the maximum discharge (charge) capacity of *ESR* e and by $(\kappa_g^e)^m$ ($(\kappa_\ell^e)^m$) the minimum discharge (charge) capacity. We refer to $(\kappa_g^e)^m.u_g^e[h]$ ($(\kappa_\ell^e)^m.u_\ell^e[h]$) and $(\kappa_g^e)^M.u_g^e[h]$ ($(\kappa_\ell^e)^M.u_\ell^e[h]$) as the *effective* lower and upper limits on the output (load) of *ESR* e such that, in any hour h, for any *ESR* $e \in \mathcal{E}$, $(\kappa_g^e)^m.u_g^e[h] \leq g^e[h] \leq (\kappa_g^e)^M.u_g^e[h]$ and $(\kappa_\ell^e)^m.u_\ell^e[h] \leq \ell^e[h] \leq (\kappa_\ell^e)^M.u_\ell^e[h]$.

Let $\epsilon^e[h]$ be the stored energy in resource $e \in \mathcal{E}$ at the *close* of hour h, or, equivalently, at the *start* of hour $[h + 1]$. This energy must satisfy the specified minimum and maximum stored energy *MWh* limits, $(\epsilon^e)^m$ and $(\epsilon^e)^M$, respectively, of *ESR* e. We also represent the discharge (charge) efficiency of *ESR* e by the factor $\eta_g^e \in (0, 1]$ ($\eta_\ell^e \in (0, 1]$). For each hour h that *ESR* e supplies $g^e[h]$ *MW* (charges $\ell^e[h]$ *MW*) to (from) the grid at its node, its stored energy level decreases (increases) by $(1/\eta_g^e)g^e[h]$ *MWh* ($\eta_\ell^e \ell^e[h]$).

B. SOP Formulation

The economic deployment of utility-scale *ESR*s aims to take advantage of arbitrage opportunities by charging the resources when electricity market prices are low and discharging their stored energy to displace electricity generated by higher-priced and, typically, polluting resources, with the overall efficiencies of the charge-discharge cycle explicitly taken into account. In this paper, we assume that each integrated *ESR* is controlled by the Independent System Operator (*ISO*), whose objective is to maximize the total system social surplus over all the hours. The *ISO*, therefore, ensures that the *ESR*s are deployed so as to enhance the economic performance of the side-by-side power system and *DAM* operations. A direct consequence of such *ESR* deployment policy is that the *ESR*s also contribute to avert uneconomical scarcity events, thereby improving the system reliability. The maximization of the system social surplus must be performed over multiple hours so as to fully take advantage of the *ESR*s' ability to shift significant amounts of energy over time. We formulate the *scheduling optimization problem* (*SOP*) to determine the most economic operational trajectory for the *ESR*s considering the variations in the demands and the outputs of the renewable resources and the available capacity of each conventional resource over the time horizon of interest. The solution of this optimization problem determines the optimal load and supply-resource dispatch, including that of the *ESR*s, for each hour of the optimization period $\overline{\mathcal{H}} = \{h : h = 1, \ldots, \overline{H}\}$. The *SOP* is formulated as a multi-period *OPF* with the explicit representation of the inter-hour constraints in storage operations, demands and supply-resource outputs, as well as the topology of the transmission network in each hour $h \in \overline{\mathcal{H}}$. In the formulation of the *SOP*, we make explicit use of the losslessness assumption typically deployed in the linearized power flow model, which is the practice in today's *ISO*-run markets [18, p. 534].

We present the mathematical statement of the *SOP* using the notation in the Appendix. For the development here, we limit the renewable resources to wind so as to simplify the presentation. The decision variables of the *SOP* are the withdrawals $\ell^b[h]$ due to each demand $b \in \mathcal{B}$, the outputs $g^s[h]$ of the various supply resources $s \in \mathcal{S}$, the operational state binary variables $u_g^e[h]$ and $u_\ell^e[h]$, the withdrawals $\ell^e[h]$, the outputs $g^e[h]$ and the stored energy level $\epsilon^e[h]$ of each *ESR* in $e \in \mathcal{E}$, as well as the phase angles $\theta_n[h]$, $\forall n \in \mathcal{N} \setminus \{0\}$, $\forall h \in \overline{\mathcal{H}}$. The *SOP* co-optimizes the withdrawal/output of each load/resource—including those of the *ESR*s—over each hour $h \in \overline{\mathcal{H}}$ with the objective to maximize the total system social surplus:

$$\max_{\substack{\ell^b[h], u_\ell^e[h], \ell^e[h], g^s[h], \\ u_g^e[h], g^e[h], \epsilon^e[h], \theta_n[h]}} \sum_{h \in \overline{\mathcal{H}}} \left[\sum_{b \in \mathcal{B}} \beta^b[h] \left(\ell^b[h]\right) - \sum_{s \in \mathcal{S}^c} \gamma^s[h] \left(g^s[h]\right) - \sum_{s \in \mathcal{S}^w} \gamma^s[h] \left(g^s[h]\right) \right] \quad (1)$$

to maximize the sum of the hourly social surpluses over the hours in $\overline{\mathcal{H}}$. The hour h social surplus is expressed as the difference between the total social benefits $\sum_{b \in \mathcal{B}} \beta^b[h](\ell^b[h])$ and the total supply costs of the conventional and wind resources, $\sum_{s \in \mathcal{S}^c} \gamma^s[h](g^s[h]) + \sum_{s \in \mathcal{S}^w} \gamma^s[h](g^s[h])$. We further assume that the cost (benefit) functions $\gamma^s(\cdot)$, $\forall s \in \mathcal{S} = \mathcal{S}^c \bigcup \mathcal{S}^w$ ($\beta^b(\cdot)$, $\forall b \in \mathcal{B}$) are piecewise linear, as is the case in the *OPF*-based market clearing mechanisms, typically, used by the *ISO*s. We explicitly exclude the benefits/costs for the storage resources in the objective function (1) as those are indirectly accounted for in terms of the *ESR* impacts on the system supply-resource dispatch costs. Indeed, in the expression for the nodal power balance equations, the term $p_n^e[h] = \sum_{e \in \mathcal{E} \text{ at node } n} (g^e[h] - \ell^e[h])$ explicitly represents the net power injection of the storage resources connected at node n in hour $h \in \overline{\mathcal{H}}$ ($g^e[h]$ and $\ell^e[h]$ cannot be both strictly positive in the same hour h, as per their effective lower and upper limits and the requirement that $u_g^e[h] + u_\ell^e[h] \leq 1$):

$$\left(\underline{p}^c[h] + \underline{p}^w[h]\right) - \underline{p}^d[h] + \underline{p}^e[h] = \underline{B}\, \underline{\theta}[h], \quad \forall h \in \overline{\mathcal{H}} \quad (2)$$

$$(p_0^c[h] + p_0^w[h]) - p_0^d[h] + p_0^e[h] = \underline{b}_0^\dagger\, \underline{\theta}[h], \quad \forall h \in \overline{\mathcal{H}}. \quad (3)$$

Each *ESR* $e \in \mathcal{E}$, whose stored energy $\epsilon^e[h-1]$ at the end of hour $[h-1]$ exceeds its minimum capability $(\epsilon^e)^m$, may act as a generation resource and displace higher-priced supply resources in hour h. In such cases, the output $g^s[h]$ of each displaced supply resource is reduced commensurately, as are their associated costs $\gamma^s[h](g^s[h])$ in the objective function (1), resulting in a corresponding increase in the social surplus (1) for that hour. For an optimal trajectory, the storage resources discharge, typically, in the peak hours so as to displace the outputs of the higher-priced supply resources and maximize the resulting increases in the objective function (1). On the other hand, when an *ESR* acts as a load to charge energy in hour h, it makes use of energy generated by both conventional and renewable resources, resulting in additional generation costs for that hour. The solution of the *SOP* takes advantage of arbitrage opportunities so that the charging hours for the storage resources are in the periods of low prices—typically, the low-load hours. The optimal solution that maximizes the total social surplus over all the hours in $\overline{\mathcal{H}}$ ensures that the *ESR*s are utilized only when the value of the energy they displace exceeds the costs incurred in their charging, with the efficiencies of the charge/discharge cycle fully taken into account. Furthermore, the optimization scheme takes advantage of the potential synergy between storage and wind resources. In the absence of storage resources, the *ISO* may be forced to "spill" wind energy due to the insufficiency of the load demand in the low-load hours. The charging of the *ESR*s may be scheduled to be carried out in such hours of high supply and low demand, when the generation costs are, typically, low. The additional demand created by *ESR* charging may be supplied, in some cases, by the wind energy that would have otherwise been "spilled". In that sense, the storage resources provide the ability to shift the wind energy produced during the low load hours to the peak load hours, when it can be used to displace the outputs of polluting and more expensive conventional resources.

The *SOP* formulation explicitly incorporates transmission constraints to ensure that the line flows do not violate the thermal limits of the transmission lines:

$$-\underline{f}^m \leq \underline{B}_d \underline{A}\theta[h] \leq \underline{f}^M, \quad \forall h \in \overline{\mathcal{H}}. \tag{4}$$

We represent of the *ESR* intertemporal operational constraints that relate the charge/discharge decisions to the stored energy in an *ESR*, with the discharge/charge efficiencies explicitly considered:

$$\epsilon^e[h] = \epsilon^e[h-1] + \frac{1}{\eta_g^e} g^e[h] - \eta_\ell^e \ell^e[h], \quad \forall h \in \overline{\mathcal{H}}, \forall e \in \mathcal{E}. \tag{5}$$

The stored energy in each hour is a critically important decision variable, even though it is not explicitly represented in (1). The presence of the constraints in (5) introduces an intertemporal coupling in the multi-hour optimization, resulting in a system of interdependent *OPF*s. These equalities serve to ensure that the storage resources accumulate energy during the lower-priced hours so as to discharge energy in subsequent, higher-priced hours. The discharge (charge) efficiency coefficient η_g^e $(\eta_\ell^e) \in (0, 1]$, strongly influence the storage resource operations. The more efficient the *ESR*s, the higher their utilization since the optimization tries to minimize the energy losses incurred with each charge/discharge cycle so as to lower the overall supply costs.

We also include the constraints to specify the capacity ranges within which an *ESR* may discharge or charge, respectively:

$$\left(\kappa_g^e\right)^m . u_g^e[h] \leq g^e[h] \leq \left(\kappa_g^e\right)^M . u_g^e[h], \ \forall h \in \overline{\mathcal{H}}, \forall e \in \mathcal{E} \tag{6}$$

$$\left(\kappa_\ell^e\right)^m . u_\ell^e[h] \leq \ell^e[h] \leq \left(\kappa_\ell^e\right)^M . u_\ell^e[h], \ \ \forall h \in \overline{\mathcal{H}}, \forall e \in \mathcal{E}. \tag{7}$$

We note that the minimum and maximum discharge (charge) capacities are both multiplied by the operational state status variable $u_g^e[h]$ $(u_\ell^e[h])$. So, whenever *ESR* e discharges (charges) in hour h, the associated status variable $u_g^e[h]$ $(u_\ell^e[h])$ is 0, resulting in the discharge output $g^e[h]$ (charge withdrawal $\ell^e[h]$) being 0. This formulation preserves the linearity of the constraints, which helps with the computational tractability.

Further, we represent constraints to ensure that an *ESR* may not both discharge and charge in the same hour h since

$$0 \leq u_g^e[h] + u_\ell^e[h] \leq 1, \quad \forall h \in \overline{\mathcal{H}}, \ \forall e \in \mathcal{E}. \tag{8}$$

$$u_g^e[h] \in \{0, 1\}, \quad u_\ell^e[h] \in \{0, 1\}, \quad \forall h \in \overline{\mathcal{H}}, \ \forall e \in \mathcal{E}. \tag{9}$$

Also, we represent the constraints on the physical limits on the energy that can be stored in *ESR* e by

$$(\epsilon^e)^m \leq \epsilon^e[h] \leq (\epsilon^e)^M, \quad \forall h \in \overline{\mathcal{H}}, \ \forall e \in \mathcal{E} \tag{10}$$

with the initial stored energy ϵ_0^e is given by

$$\epsilon^e[0] = \epsilon_0^e, \quad \forall e \in \mathcal{E}. \tag{11}$$

The consideration of the limits on the demand/output of all each load and each supply resource results in the constraints:

$$0 \leq \ell^b[h] \leq d^b[h], \quad \forall h \in \overline{\mathcal{H}}, \quad \forall b \in \mathcal{B} \tag{12}$$

$$(\kappa^s)^m \leq g^s[h] \leq a^s[h], \quad \forall h \in \overline{\mathcal{H}}, \quad \forall s \in \mathcal{S}^c \tag{13}$$

$$0 \leq g^s[h] \leq w^s[h], \quad \forall h \in \overline{\mathcal{H}}, \quad \forall s \in \mathcal{S}^w. \tag{14}$$

The resulting *SOP* in (1)–(14) is a large-scale mixed-integer linear program (*MILP*). We use the superscript * to denote the optimal value of the decision variables that solve the *SOP*. For example, the $(g^e)^*[h]$ $((\ell^e)^*[h])$ values provide the *ESR* dispatch results $\forall e \in \mathcal{E}$, $\forall h \in \overline{\mathcal{H}}$. We note that the solution to the *SOP* determines not only the operations of the *ESR*s, but also the load and resource dispatch for each hour in the optimization period. Similarly, at the optimum, the dual variables (shadow prices) of the power balance constraints (2) and (3) are interpreted as the locational marginal prices (*LMP*s) for each hour $h \in \overline{\mathcal{H}}$. As such, we view the dispatch and shadow prices determined by the *SOP* solution to be those of a *DAM* with the explicit representation of the impacts of the *ESR*s on the nodal net power injections, and consequently, on the *DAM* outcomes. We make use of this fact in the extension of the stochastic simulation approach of [5] to represent the impacts of the utility-scale storage resources on the side-by-side power system and market operations. We also note that, absent the representation of the *ESR*s and their associated intertemporal coupling constraints (5), the *SOP* consists of H separate *OPF* problems that may then be independently solved. Each such *OPF* is identical to the

hourly *DAM* clearing model discussed in the Appendix in [5]. Thus, the *SOP* can be seen as the "time-coupled", generalized statement of the *DAM* clearing problem formulated in [5].

In the next section, we discuss the *SOP* deployment in the extended simulation approach to determine not only the schedule but to also emulate the clearing of the *DAM*s with integrated storage resources.

III. Extended Stochastic Simulation Approach

We devote this section to the discussion of the steps undertaken to incorporate the representation of the utility-scale *ESR*s into the stochastic simulation approach for power systems with integrated renewable resources presented in [5]. We use the simulation we developed to emulate the side-by-side power system and transmission-constrained *DAM* operations with the objective to quantify the impacts of integrated renewable resources on the power system variable effects over longer duration periods. We briefly review such stochastic simulation approach in the first subsection, then discuss in the second subsection its extension to incorporate the representation of *ESR*s.

A. Fundamentals of the Stochastic Simulation Approach

The simulation study period $\mathcal{T}$ is decomposed into the non-overlapping weekly simulation periods $\mathcal{T}_i$'s with $\mathcal{T} = \bigcup_i \mathcal{T}_i$, $\mathcal{T}_i \bigcap \mathcal{T}_j = \varnothing$. We assume the system resource mix and unit commitment, the transmission grid, the operational policies, the market structure and the seasonality effects are fixed over the duration of each simulation period $\mathcal{T}_i$. Each simulation period consists of 168 hourly subperiods, whose set is denoted by $\mathcal{T}_i = \{h : h = 1, \ldots, 168\}$, and where each subperiod h is the smallest indecomposable unit of time in the representation of any phenomena of interest.

For the explicit consideration of uncertainty associated with the time-varying loads, the highly variable renewable resources and the available capacities of the conventional resources, we use discrete-time random processes (*r.p.s*) indexed by the 168 hours of the simulation period. Each conventional resource is modeled as a multi-state unit with two or more states—outaged, various partially derated capacities and full capacity. We assume that each conventional resource is statistically independent of any other generation resource, and use a discrete-event driven Markov Process model with the appropriate stochastic event-times distributions to represent the underlying *r.p.* governing the available capacity of each conventional resource [19]. The modeling of the multi-site wind speed and demand share some similarities: we make use of time-synchronized mesoscale data to construct the wind speed (power output) and demand input *r.p.s*.[2] More specifically, we gather weeks of simultaneously-measured hourly wind speeds at multiple sites buyer demands (at multiple buses) from time-synchronized mesoscale historical data. We use these data to build the sample spaces of wind speed and demand random processes and capture, as a result, the spatial and time correlations among the hourly wind speeds (demands) at multiple sites (load buses). In particular, the multi-site wind speed (nodal buyer demand) random process is a collection of time-indexed random vectors, with each random vector containing the ordered collection of the wind speed (buyer demand) random variables at the multiple sites (load buses) for each value of the time index, i.e., a particular sub-period of the simulation. We note that, by construction from the time-synchronized mesoscale data, the random variables that are the elements of the time-indexed random vectors in the collection that represents the random process of interest, be it the nodal demand or multi-site wind speed random process, are intrinsically correlated. The random process representation, therefore, captures the time dependent behavior of the wind speeds (wind resource outputs) at the various locations and that of the nodal demands. Under this representation, in a system with low winds during peak load periods for example, the expected high demand in a peak hour h is associated with low expected values in the wind power outputs in that same hour h. In this way, our approach represents the misalignment of the wind power outputs and the demand in such a peak hour h. We use the simplifying assumption that the random variable that represents the wind speed at site i in hour h and the random variable that represents the nodal buyer b demand in hour h are statistically independent. This assumption, in effect, indicates that the behavior of buyer b demand in hour h has no impact on the behavior of the site i wind speed (power output) in that hour and in all the other hours and vice-versa. In terms of the misaligned wind power outputs and loads during peak hour h example discussed above, the statistical independence assumption implies that the deviations of the wind power outputs from their low expected values in peak hour h are independent from the deviations of the demands from their high expected values in that same peak hour h. In some other hours, both the wind and demand may be low—and this will be correctly represented by our approach since the expected values of the wind and demand random variables in those hours will be low—yet their deviations around their expected values will be independent. We note that this statistical independence assumption is reasonable in light of the primary purpose of our simulation approach: to evaluate, over longer-term periods, the expected variable effects of large-scale power systems with integrated renewable and storage resources. As such, our methodology does not represent the more extreme and exceptional weather events such as storms, for example, that may strongly impact—albeit over relatively short-term periods—both demand and wind patterns. Furthermore, in the study of large scale systems, we note that the wind resources are often located at considerable distance from the load centers. Under such conditions, the hourly wind speed variations at a remote wind farm are unrelated to the hourly variations in the demands, and so the correlations among demands and wind speeds, or, equivalently, power outputs are, virtually, 0. Thus, for such simulations, it is reasonable to assume that the demands behave independently from the wind speeds (power outputs).

In the analytical framework of the approach, we view the hourly transmission-constrained *DAM* outcomes as the mapping of the "input" *r.p.s* via the *OPF* solution of the market clearing. Consequently, the *DAM* outcomes are also *r.p.s* indexed by the 168 hours of the simulation period. For convenience, we refer to

[2]We note that any statement on the wind speed *r.p.* applies equally well to a statement on its associated wind power output *r.p.* due to the fact that the wind power output is modeled as a piece-wise polynomial function of the wind speed.

them as the "output" *r.p.s*. The approach's use of Monte Carlo simulation techniques systematically samples the various *r.p.s* to generate the so-called *sample paths* (*s.p.s*) that contain the hourly realizations of the random variables (*r.v.s*) constituting the *r.p.s*. The thrust of the Monte Carlo simulation approach is the emulation of the 168 hourly *DAM* outcomes in each simulation period. The *s.p.s* of the input *r.p.s* provide the basis for the formulation of the offers and bids into the 168 *DAM*s of the simulation period. The clearing of the 168 *DAM*s in the simulation period results in the construction of the *s.p.s* of the output *r.p.s*. We refer to the evaluation of the hourly *DAM* outcomes for the 168 hours in the simulation period as a simulation run. The basic idea of the *independent* Monte Carlo simulation [20, p. 10] is to execute multiple statistically independent simulation runs in such a way as to construct for each "output" *r.p.* of interest a collection of output *s.p.s* which are used to estimate the performance metrics. Such performance metrics are selected to be the expected values of the time-indexed *r.v.s* constituting the output *r.p.s* of interest.[3] We perform a sufficient number of simulation runs to obtain the specified statistical reliability requirement for the sample mean estimators of the market outcomes of interest [21, pp. 82 and 451].

B. Extension of the Approach To Represent the ESRs

We now detail the steps taken to extend the base stochastic simulation framework summarized in Section III-A to incorporate the representation of the utility-scale *ESR*s. With the intertemporal coupling introduced by the representation of the *ESR* operations, we can no longer solve, as part of a simulation run, a sequence of 168 independent hourly *OPF*s to clear the hourly *DAM*s over the week-long simulation period. By contrast, we now solve a sequence of 7 *SOP*s, one for each day of the week. In such a context, each *SOP* serves two purposes: to emulate, for a given day in the simulation period $\mathcal{T}_i$, the clearing of its 24 hourly *DAM*s, and to schedule the *ESR* operations over a week-long period whose first day is the day whose *DAM* clearing results are obtained. For clarity in the presentation, we will refer to such a day as day j in the simulation period $\mathcal{T}_i$, with $j \in \{1, \ldots, 7\}$. We regard the solutions of the *SOP* for the 24 hours of day j to be the outcomes of the corresponding hourly *DAM*. These day j outcomes serve to construct the output *s.p.s* whose values we use to quantify the performance metrics of interest. The *SOP* optimization period $\overline{\mathcal{H}} = \{h : h = 1, \ldots, \overline{H}\}$ must also include additional hours that immediately follow the 24 hours of day j to ensure that the *ESR*s are scheduled in such a way as to reflect their continued operations beyond the simulated day j. Such additional period is required so that the *ESR*s are not discharged by the last hour of day j, an unrealistic outcome as the *ESR*s are operated on a broader horizon than a day. To avoid complications with a limited scheduling horizon, we solve each *SOP* over a week-period and so $\overline{H} = 168$ for a given simulation period $\mathcal{T}_i$. The solution of each *SOP* for the hours beyond those of the simulated day j are *not* used in the construction of the output *s.p.s*; they serve simply to represent the continued operations of the *ESR*s

[3]Other metrics, such as the variances of said *r.v.s*, may be defined along similar lines.

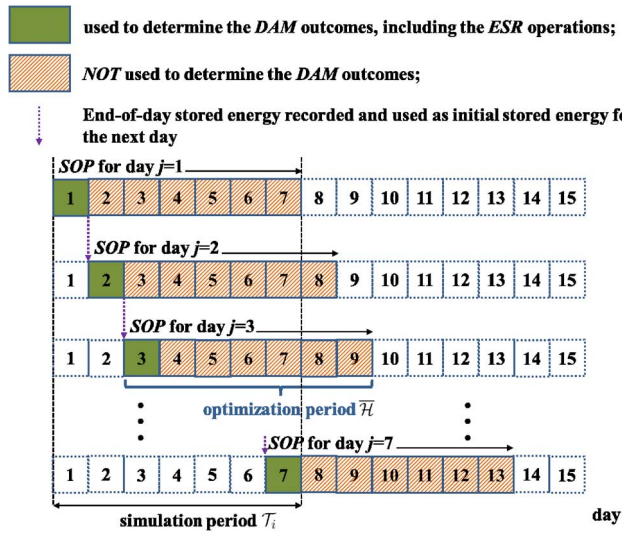

Fig. 1. Role of the *SOP* in the emulation of the *DAM*s of a simulation period.

beyond day j. The stored energy of each *ESR* at the end of the last hour of day j is recorded to be used as the initial stored energy of each *ESR* in the formulation of the *SOP* for the day $(j+1)$. For the purposes of this discussion, we assume that the initial stored energy level ϵ_0^e of each *ESR* $e \in \mathcal{E}$ in the first hour of day 1 is given. For each hour h in day j, the so-called cost (benefit) functions $\gamma^s(\cdot)$, $\forall s \in \mathcal{S} = \mathcal{S}^c \bigcup \mathcal{S}^w$ ($\beta^b(\cdot)$, $\forall b \in \mathcal{B}$) in the *SOP* objective (1) are the offer (bid) functions submitted by each seller (buyer) for the 24 *DAM*s of day j. The upper bounds on the demands in (12) and the supply-resource outputs in (13) and (14) are set by the hourly realizations of the *s.p.s* of the corresponding input *r.p.s*, as is the case discussed in [5]. The sampling procedure we use to construct such *s.p.s* from the joint cumulative distribution functions of the corresponding input *r.p.s* is identical to that in [5]. For each hour h beyond the 24 hours of day j, the offer (bid) functions, as well as the upper bounds on the demands and supply-resource outputs are obtained differently to reflect the fact that, in the real world, the market players only submit their bids and offers for the "current" day j and any supplementary information about the hours following day j must be estimated by the *ISO*. Thus, we assume that the demands are fixed and the sellers offer at a predetermined price in all hours following day j; furthermore, we make use of the expected values for the loads and wind power outputs, coupled with the assumption that a conventional generation resource keeps running at full capacity (potentially after recovering from a forced outage state) to determine the upper bounds on the demands and supply-resource outputs in these hours. We illustrate in Fig. 1 the overall procedure for the execution of a given simulation run.

In terms of the stochastic simulation framework, the *ESR*'s operating outputs are represented by a discrete-time *r.p.*, along the lines used to represent the uncertain and time-varying demands or multi-site wind speeds in [5]. As such, the *ESR* operation *r.p.* is a collection of time-indexed random vectors for $h \in \mathcal{T}_i$, where each random vector in a given hour h contains the *r.v.s* that represent the output of each *ESR* in $\mathcal{E}$. Such model

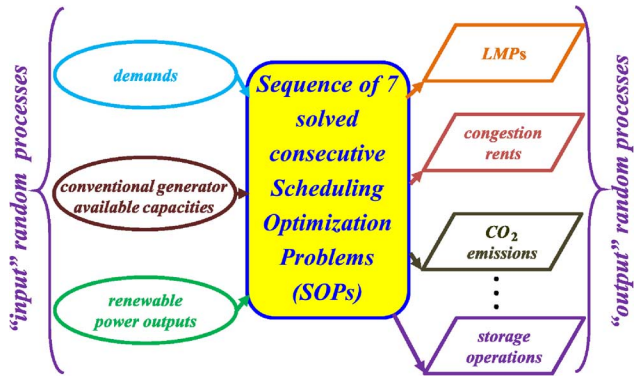

Fig. 2. Conceptual structure of the simulation approach with the incorporated utility-scale storage resources.

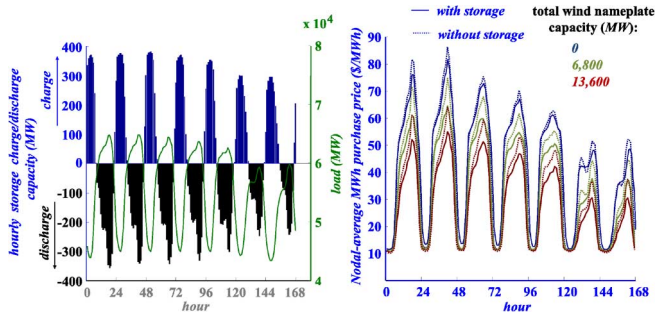

Fig. 3. Expected hourly storage operation and *SMP*s.

captures the cross-correlations among the operations of the various *ESR* in $\mathcal{E}$ as well as the correlations over time that characterize the strongly time-dependent behaviors of storage resources. Within the framework of our extended simulation approach, the storage operation *r.p.* constitutes an output *r.p.* that is obtained from the mapping of the input *r.p.s*—the buyer demand, the multi-site wind speed and the conventional generation resource available capacity *r.p.s*—by the sequence of the 7 *SOP* solutions. As shown in Fig. 2, the other output *r.p.s* are the same as in [5].

We also discuss the use of a relaxed version of the *SOP* in (1)–(14) for improved tractability in the Monte Carlo simulations. We relax the highly-computationally-intensive *MILP* into the more tractable linear program (*LP*) we next describe. The proposed relaxation only involves the modification of constraints (6) and (7): we assume that the *ESR* minimum charge $(\kappa_\ell^e)^m$ and discharge $(\kappa_g^e)^m$ capacities are 0, with all the binary variables u_g^e and u_ℓ^e equal to 1. We note that the outcomes of the resulting *LP* cannot reflect the impacts of the *ESR* minimum discharge/charge capacities. In actual simulations, the discharge outputs (charge loads) that fall below the minimum charge $(\kappa_\ell^e)^m$ (discharge $(\kappa_g^e)^m$) capacities can be approximated by simply rounding them to either 0 (in which case, such *ESR*s would be considered idle) or said minimum discharge (charge) capacities, whichever is closer. We found that the proposed relaxation proved effective in the case studies reported in Section IV, as there were very few hours for which such rounding was necessary.

In the next section, we illustrate the broad capabilities of the extended stochastic simulation approach with a variety of case studies aimed at investigating the economic, reliability and emission impacts of integrated *ESR* in power systems with integrated wind resources.

IV. Representative Simulation Results

We performed extensive testing of the simulation approach on various test systems to study a broad range of applications, including resource planning, production costing issues, transmission planning, environmental assessments, reliability and policy analysis. We illustrate the application of the approach with three representative studies performed on modified *IEEE* 118 [22] and *WECC* 240-bus systems [23]. We refer the reader to [24] and [5] for the detailed description of the modified *IEEE* 118 and *WECC* 240-bus systems, respectively. In all the case studies, we run a unit commitment for each simulation period to determine the set of conventional generators that are committed, and so, the sellers that participate in the *DAM*s, and ensure a 15% reserve margin (unless otherwise specified), measured with respect to the simulation period peak load. In such cases where *ESR*s are part of the resource mix, we assume that each *ESR* reserve capability is equal to its installed capacity, in light of the ability of *ESR*s to discharge and thereby provide capacity during the peak hours. As a result, each *MW* of installed *ESR* capacity replaces a *MW* of conventional generation capacity to meet the 15% reserves requirements in systems with *ESR*s in the resource mix. We note, however, that were a co-optimized energy/ancillary service market implemented, such an assumption would no longer be necessarily valid since the market clearing would determine which resources are to provide capacity for the purpose to meet the 15% reserves requirements. We also assume that each buyer bids his load as a *fixed* demand in each hourly *DAM*. Since wind power has no fuel costs, we assume that all wind power outputs are offered at 0 *$/MWh* in each hourly *DAM* throughout the simulation period. In each study, we limit our analysis to a single year in order to focus on the insights into the nature of the results obtained. Thus, all chronological plots are done over the "average week of the year", for which the hourly values are averaged over all the representative weeks of the year [5], with weights equal to the number of actual weeks represented by each represented week.

In the first case study, we examine the impacts of integrated *ESR*s on the modified *WECC* 240-bus system under deepening wind penetration: from 0 *MW* total wind nameplate capacity in the base case to 13 600 *MW*, in 3400 *MW* increments. The total wind nameplate capacity is allocated in equal quantities among 4 wind farms at distinct locations. To gain insights into the impacts of the integrated *ESR*s on the variable effects, we evaluate each wind penetration case with and without the *ESR*s. In the no storage cases, the supply-side resources consist of the system conventional generation units and the 4 wind farms, while operations use a 15% reserves margin provided solely by the conventional units. In the storage cases, the system sports, in addition to the resource mix of the no storage cases, 5 identical storage units, each with 400 *MW* capacity, 4000 *MWh* storage capability and a round-trip efficiency of 0.9. In such cases, the

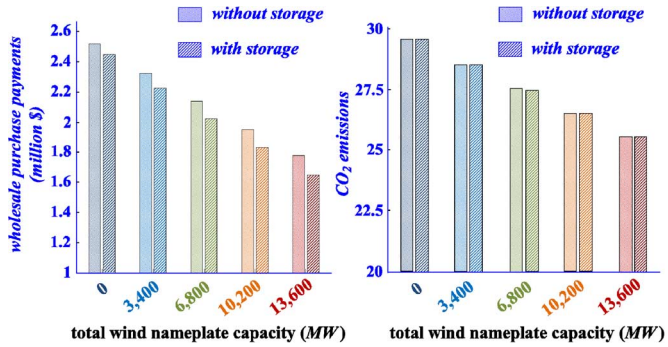

Fig. 4. Expected hourly total wholesale purchase payments and CO_2 emissions; all values are averages over the hours of the year.

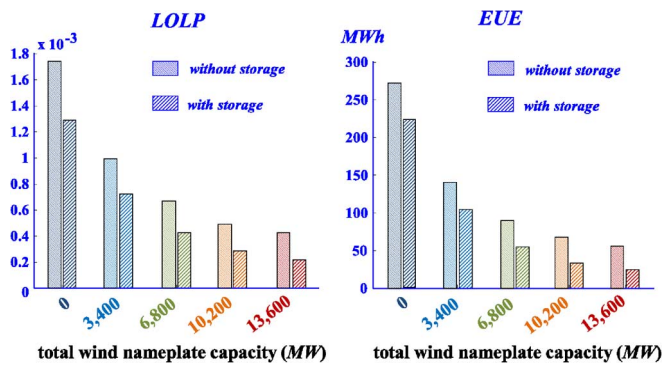

Fig. 5. Annual reliability metrics.

15% reserves margin is provided by a combination of conventional and storage resources. We provide in Fig. 3 plots of the expected hourly storage charge load/discharge output for one of the *ESR*s, as well as the expected hourly values of what we call, for convenience, the *system marginal prices* (*SMP*s)—the weighted averages of the *LMP*s over all the system nodes, with weights equal to the cleared demands.

The results indicate that the *ESR*s tend to charge (discharge) during the low-load (peak-load) hours when the electricity prices are low (high). The *SMP* plots further show that the *ESRs* not only favorably impact the peak-load hour prices, they also reinforce the benefits brought about by integrated wind resources. We note from the plots in Fig. 4 that, as the wind penetration deepens, the expected hourly total wholesale purchase payments and CO_2 emissions are reduced. Significant improvements in the system reliability indices are shown in Fig. 5. These plots also make plainly clear that these reductions and improvements are characterized by diminishing returns as the wind penetration deepens. Such results are representative of the ability of the *ESR*s to attenuate, to some extent, such diminishing returns. Overall, storage works in synergy with wind to drive down further wholesale purchase payments and improve system reliability. On the other hand, CO_2 emissions are insignificantly affected by the integration of a storage unit. We attribute this result to the fact that, in a system where the nameplate wind capacity does not exceed the system base load, CO_2 emissions depend largely on the relative utilization of the various fossil-fuel fired units, as affected by the charge/discharge cycles of the *ESR*s. In this particular case, the reductions

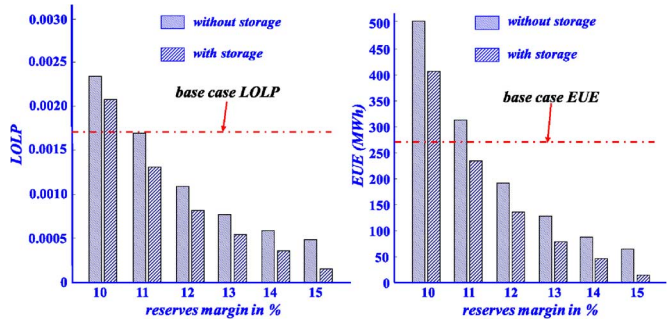

Fig. 6. Annual *LOLP* and *EUE* versus system reserves margins.

in CO_2 emissions caused by the *ESR* displacement of polluting conventional resources during the peak-load hours are about the same as the increases in CO_2 emissions due to *ESR* charging during the low-load hours.

In the second case study, we investigate the extent to which a combination of wind and *ESR*s may replace conventional resources from a purely system reliability perspective in the *WECC* 240-bus system. For reference, we also provide the results of the same case study with no *ESR*s. The base case with no wind and no *ESR*s evaluates the system *LOLP* and *EUE* with a 15% system reserves margin. In all the other cases, the conventional resource mix is supplemented by 4 wind farms—with a total nameplate capacity of 13 600 *MW*, i.e., about 16% of the annual 81 731 *MW* peak load - and 5 identical storage units as in the first study set. In these cases, the reserves are provided by the conventional *and ESR*s (where applicable) and we examine the impacts of progressively retiring some conventional resources, thus decreasing reserves margin levels. We provide in Fig. 6 the annual *LOLP* and *EUE* values as a function of the system reserves margin levels.

The sensitivity results without *ESR*s indicate that the 13 600 *MW* of installed wind capacity can replace roughly 4% of the weekly peak loads, on average over the year, in terms of retired conventional generation capacity, that is about 3000 *MW*. With the integrated *ESR*s, and all other conditions unchanged, the *LOLP* results indicate that another half percent can be replaced, which corresponds to an additional 400 *MW* of retired conventional generation capacity. We note that, as the reserves are provided by the conventional *and ESR*s, these additional 400 *MW* represent the added benefits, from a purely reliability perspective, of combining wind and storage resources. While the wind resources by themselves had a firm capacity of about 22% of their total nameplate capacity, the integration of 2000 *MW* of storage capacity raised the wind resource firm capacity by an additional 3% of the total wind nameplate capacity. This result indicates that wind and *ESR*s can work synergystically to improve system reliability.

The third case study pinpoints the ability of the simulation approach to study congestion impacts. We examine the impacts of *ESR* siting on transmission utilization and the economics of node 59, the most heavily loaded bus in our modified *IEEE* 118-bus test system. We present sensitivity cases that involve the siting of 4 identical *ESR*s—each with 200 *MW* capacity, 2000 *MWh* storage capability and a round-trip efficiency of

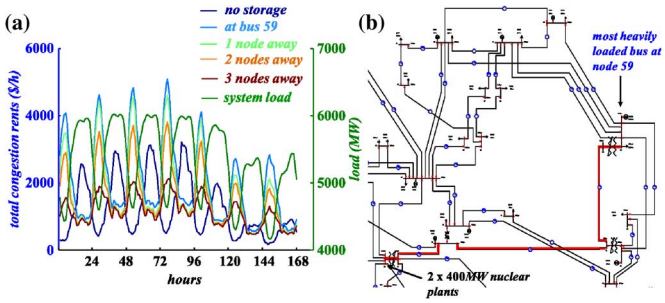

Fig. 7. Expected hourly total congestion rents (a) and transmission path congestion (b).

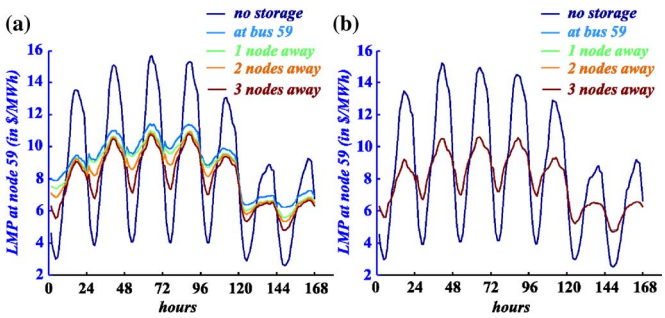

Fig. 8. Expected hourly LMP at bus 59 before (a) and after doubling the transmission capacity of the path (b).

0.9—as the *ESR*s are successively further removed from bus 59. The total *ESR* capacity accounts for about 10% of the annual peak load. For reference, we provide a base case with no integrated *ESR*s. In the first subcase, all the 4 *ESR*s are located at bus 59. In each subsequent subcase, the *ESR*s are sited one more node removed from bus 59, such that in the 4th subcase, all *ESR*s are 3 nodes away from bus 59. We provide in Fig. 7 plots of the expected hourly total congestion rents as well as what we have identified to be a congested transmission path, from a major generation source node with 2 nuclear 400 *MW* units to the major load center at bus 59.

The congestion rent plots in Fig. 7(a) indicate that *ESR* operations cause congestion during the low-load hours, especially so the closer to bus 59 the *ESR*s are sited. We provide in Fig. 8(a) plots of the expected hourly *LMP*s at bus 59 that incorporate the impacts of such congestion. For each siting subcase, the congestion rents are clearly reflected in the bus 59 *LMP* and particularly so during the low-load hours. These plots further indicate the influence of siting the *ESR*s on the decreases (increases) of bus 59 *LMP* during the high-load (low-load) hours due to *ESR* discharge to displace more expensive conventional resources (charge). The observed congestion leads to an examination of effective steps to reduce the congestion rents. For example, the increase of the total transmission capacity of the path (depicted in Fig. 7(b)) by 100% results in the elimination of the congestion and in virtually identical *LMP*s for each siting subcase, as shown in Fig. 8(b). The results also indicate that, in this particular case study, it is best to locate the *ESR*s 3 nodes away from bus 59 in order to avert the transmission path congestion and the resulting raise in bus 59 *LMP*. Indeed, the curves in Fig. 8(b) are essentially the same as the curve in Fig. 8(a) representing the evolution of bus 59 *LMP* before the reinforcement of the transmission path and when the *ESR*s are 3 nodes removed from bus 59. Overall, this third case study suggests that the siting of *ESR* can have significant impact on the network congestion patterns and, consequently, on the *LMP*s.

V. Conclusion

In this paper, we report on the extension of a stochastic simulation approach for power system with integrated renewable resources to incorporate the representation of utility-scale energy storage resources. We develop models for the energy storage resources and deploy the scheduling optimization problem to schedule their operations over multiple time periods, in conjunction with the demands and the conventional/renewable resources and with the explicit consideration of the transmission constraints. The seamless incorporation of the energy storage resource representation into the stochastic simulation approach allows us to retain the detailed use of discrete-time random processes in the adaptation of Monte Carlo simulation techniques to explicitly represent the various sources of uncertainty in the demands, the available capacity of conventional generation resources and the time-varying renewable resources, with their temporal and spatial correlations. In such a framework, the energy storage resource operations are themselves represented by a discrete-time random process, as their operations directly depend on the interactions among the demands and other supply-resources. The extended simulation approach thus sports the ability to quantify the impacts of integrated renewable and storage resources on the power system economics, reliability and emissions.

The representative results we present from the extensive studies performed demonstrate effectively the strong capabilities of the simulation approach. The results of these studies on modified *IEEE* 118 and *WECC* 240-bus systems, clearly indicate that energy storage and wind resources tend to complement each other and this symbiosis reduces wholesale costs and improves system reliability. In addition, we observe that emission impacts with energy storage depend on the resource mix characteristics. An important finding is that storage seems to attenuate the "diminishing returns" associated with increased penetration of wind generation. The limited ability of integrated storage resources to enhance the wind resource capability to substitute for conventional resources from purely a system reliability perspective is evidenced in the studies presented. Some useful insights into the siting of storage resources are obtained and they indicate the potentially significant impacts of such decisions on the network congestion patterns and, consequently, on the *LMP*s.

The development of the approach provides the first comprehensive implementation for the simulation of large-scale power systems with integrated renewable and storage resources. The stochastic simulation approach has a broad range of applications to various issues in planning, operational analysis, investment evaluation, policy formulation and analysis and provides quantitative answers to various *what if* questions.

APPENDIX

Notation:

$[h]$	Discrete time variable (hour).
$\overline{\mathcal{H}} = \{h : h = 1 \ \ldots \ \overline{H}\}$	Optimization period of the *SOP*.
$\mathcal{N} = \{n : n = 0, 1, \ldots, N\}$	Set of network buses with bus 0 as the slack bus. We consider the network consists of $N+1$ buses.
$\mathcal{L} = \{(i,j) : i \in \mathcal{N},\ j \in \mathcal{N},\ i \text{ and } j \text{ are connected}\}$	Set of transmission lines.
$\underline{A}$	Reduced branch to node incidence matrix.
$\underline{B}_d$	Branch susceptance matrix.
$\underline{B}$	Reduced nodal susceptance matrix.
$\underline{b}_n$	Column vector of the nodal susceptance matrix corresponding to bus n.
$\underline{\theta} = [\theta_1, \theta_2, \ldots, \theta_N]$	Vector of power angle (excluding the slack bus power angle which is taken as 0).
$\underline{f} = \underline{B}_d \ \underline{A} \ \underline{\theta}$	Vector of line flows.
$\underline{f}^M$	Vector of transmission line thermal rating.
$\underline{f}^m$	Vector of transmission line thermal rating in the opposite flow direction.
$\mathcal{S}^w$	Set of wind farms that participate in the *DAM*.
$\mathcal{S}^c$	Set of conventional generation resources that participate in the *DAM*.
$\mathcal{S} = \mathcal{S}^w \bigcup \mathcal{S}^c$	
γ^s	Offer price of seller s.
g^s	Seller s resource output (decision variable).
a^s	Available capacity of seller s generation resource.
w^s	Available power output of seller s wind farm.
$(\kappa^s)^m$	Minimum capacity of seller s generation resource.
$p_n^c = \sum_{s \in \mathcal{S}^c \text{ is at node } n} g^s$	Power injection at node n due to conventional resource generation.
$p_n^w = \sum_{s \in \mathcal{S}^w \text{ is at node } n} g^s$	Power injection at node n due to wind farm generation.
$\mathcal{B}$	Set of buyers in the *DAM*.
β^b	Buyer b willingness-to-buy.
ℓ^b	Buyer b demand (decision variable).
$p_n^d = \sum_{b \in \mathcal{B} \text{ is at node } n} \ell^b$	Power consumption at node n due to loads.
$\mathcal{E}$	Set of *ESR*s being considered.
g^e	*ESR* e output (decision variable).
$p_n^e = \sum_{e \in \mathcal{E} \text{ is at node } n} (g^e - d^e)$	*net* power injection at node n due to *ESR* generation/consumption.
u_g^e	*ESR* e discharge status (binary) variable.
u_ℓ^e	*ESR* e charge status (binary) variable.
$(\kappa_g^e)^M$	Maximum discharge capacity of *ESR* e.
$(\kappa_g^e)^m$	Minimum discharge capacity of *ESR* e.
η_g^e	Discharge efficiency of *ESR* e.
$\epsilon^e[h]$	*ESR* e stored energy at the end of hour h.
ℓ^e	*ESR* e demand (decision variable).
$(\kappa_\ell^e)^M$	Maximum charge capacity of *ESR* e.
$(\kappa_\ell^e)^m$	Minimum charge capacity of *ESR* e.
η_ℓ^e	Charge efficiency of *ESR* e.
$\eta^e = \eta_\ell^e . \eta_g^e$	Round-trip efficiency of *ESR* e.
x^*	Optimal value of decision variable x in the *SOP*.
$\mathcal{T} = \bigcup_i \mathcal{T}_i$	Study period.
$\mathcal{T}_i$	*i*th simulation period.
$\mathcal{T}_i = \{h : h = 1, \ldots, H\}$	Set of subperiods h, i.e., smallest indecomposible unit of time, in a simulation period $\mathcal{T}_i$; in the proposed application of the approach, a subperiod is of duration one hour and $H = 168$.

REFERENCES

[1] P. Denholm, E. Ela, B. Kirby, and M. Milligan, "The role of energy storage with electricity renewable generation," NREL, Tech. Rep., 2010 [Online]. Available: http://www.nrel.gov/docs/fy10osti/47187.pdf

[2] D. Rastler, "Electricity energy storage technology options—a white paper primer on applications, costs and benefits," EPRI, Tech. Rep., 2010 [Online]. Available: http://large.stanford.edu/courses/2012/ph240/doshay1/docs/EPRI.pdf

[3] Electricity Advisory Committee, "Bottling electricity: Storage as a strategic tool for managing variability and capacity concerns in the modern grid," DOE, Tech. Rep., 2008 [Online]. Available: http://energy.gov/sites/prod/files/oeprod/DocumentsandMedia/final-energy-storage_12-16-08.pdf

[4] I. Gyuk *et al.*, "Grid energy storage," U.S. Department of Energy, Tech. Rep., 2013 [Online]. Available: http://energy.gov/sites/prod/files/2013/12/f5/Grid%20Energy%20Storage%20December%202013.pdf

[5] Y. Degeilh and G. Gross, "Stochastic simulation of power systems with integrated intermittent renewable resources," *Int. J. Elect. Power Energy Syst.*, accepted for publication.

[6] J. Himelic and F. Novachek, "Sodium sulfur battery energy storage and its potential to enable further integration of wind (wind-to-battery project)," Xcel Energy, Tech. Rep., 2011 [Online]. Available: http://www.xcelenergy.com/staticfiles/xe/Corporate/Renewable Energy Grants/Milestone6FinalReport PUBLIC.pdf

[7] Y. Yuan, Q. Li, and W. Wang, "Optimal operation strategy of energy storage unit in wind power integration based on stochastic programming," *IET Renew. Power Gener.*, vol. 5, no. 2, pp. 194–201, Mar. 2011.

[8] B. Hartmann and A. Dan, "Cooperation of a grid-connected wind farm and an energy storage unit—Demonstration of a simulation tool," *IEEE Trans. Sustain. Energy*, vol. 3, no. 1, pp. 49–56, Jan. 2012.

[9] M.-S. Lu, C.-L. Chang, W.-J. Lee, and L. Wang, "Combining the wind power generation system with energy storage equipment," *IEEE Trans. Ind. Applicat.*, vol. 45, no. 6, pp. 2109–2115, Nov. 2009.

[10] R. Walawalkar and J. Apt, "Market analysis of emerging electric energy storage systems," DOE/NETL, Tech. Rep., 2008.

[11] S. Tewari and N. Mohan, "Value of NaS energy storage toward integrating wind: Results from the wind to battery project," *IEEE Trans. Power Syst.*, vol. 28, no. 1, pp. 532–541, Feb. 2013.

[12] S. Gill, E. Barbour, I. Wilson, and D. Infield, "Maximising revenue for non-firm distributed wind generation with energy storage in an active management scheme," *IET Renew. Power Gener.*, vol. 7, no. 5, pp. 421–430, Sep. 2013.

[13] H. Akhavan-Hejazi and H. Mohsenian-Rad, "Optimal operation of independent storage systems in energy and reserve markets with high wind penetration," *IEEE Trans. Smart Grid*, vol. 5, no. 2, pp. 1088–1097, Mar. 2014.

[14] G. Hug-Glanzmann, "Coordination of intermittent generation with storage, demand control and conventional energy sources," in *Proc. 2010 IREP Symp.—Bulk Power System Dynamics and Control—VIII*, Buzios, Rio de Janeiro, Brazil, Aug. 1–6, 2010.

[15] J. Lee, J.-H. Kim, and S.-K. Joo, "Stochastic method for the operation of a power system with wind generators and superconducting magnetic energy storages (smess)," *IEEE Trans. Appl. Supercond.*, vol. 21, no. 3, pp. 2144–2148, Jun. 2011.

[16] J. Deane, E. McKeogh, and B. Gallachoir, "Derivation of intertemporal targets for large pumped hydro energy storage with stochastic optimization," *IEEE Trans. Power Syst.*, vol. 28, no. 3, pp. 2147–2155, Aug. 2013.

[17] C. Murillo-Sanchez, R. Zimmerman, C. Lindsay Anderson, and R. Thomas, "Secure planning and operations of systems with stochastic sources, energy storage, active demand," *IEEE Trans. Smart Grid*, vol. 4, no. 4, pp. 2220–2229, Dec. 2013.

[18] A. Wood and B. Wollenberg, *Power Generation, Operation and Control*. New York, NY, USA: Wiley, 1996.

[19] "Markov models for reliability evaluation (notes for ECE 588 UIUC)." [Online]. Available: http://courses.engr.illinois.edu/ece588/handouts/Lecture3-MarkovModelsforReliabilityEvaluation.pdf

[20] G. Fishman, *A First Course in Monte Carlo*. Pacific Grove, CA, USA: Duxbury, 2006.

[21] J. Kleijnen, *Statistical techniques in simulation—Parts 1 and 2*. New York, NY, USA: Marcel Dekker, Inc, 1974.

[22] "118-bus Power Flow Test Case." [Online]. Available: http://www.ee.washington.edu/research/pstca/pf118/pg_tca118bus.htmD

[23] J. Price and J. Goodin, "Reduced network modeling of*WECC* as a market design prototype," in *Proc. IEEE PES General Meeting*, Detroit, MI, USA, Jul. 24–28, 2011, pp. 1–6.

[24] Y. Degeilh and G. Gross, "Integration of storage devices into power systems with renewable energy sources—Part 1: Simulation of energy storage in a system with integrated wind resources," S-40 final project report, PSERC publication 12-24, Tech. Rep., 2012 [Online]. Available: http://www.pserc.wisc.edu/documents/publications/reports/2012_reports/

Yannick Degeilh has recently defended his Ph.D thesis in power system engineering at the University of Illinois at Urbana-Champaign and is currently serving as a consultant for Energy Exemplar LLC—the developers of the Energy Market Modeling software PLEXOS—in Roseville, California. Yannick also holds a M.Sc. degree from Texas A&M University in the same area of expertise and received his French engineer degree in Mechanical/Electrical Engineering from the Ecole Spéciale des Travaux Publics (ESTP), Paris, France. His research interests include power system analysis, planning and operations, energy markets, renewable resource integration as well as stochastic modeling, simulation and optimization.

George Gross (F'88) is Professor of Electrical and Computer Engineering and Professor, Institute of Government and Public Affairs, at the University of Illinois at Urbana-Champaign. His current research and teaching activities are in the areas of power system analysis, planning, economics and operations, utility regulatory policy and industry restructuring. In the 1999–2000 academic year, he was a Visiting Professor at a number of Italian institutions of higher learning, including University of Pavia, Politecnico di Milano and Politecnico di Torino. His undergraduate work was completed at McGill University, and he earned his graduate degrees from the University of California, Berkeley. He was formerly with the Pacific Gas and Electric Company, where Dr. Gross founded the company's Management Science Department and held other key management, technical and policy positions. During 1992–93, Dr. Gross was at the Electric Research Power Institute to develop research directions on open access transmission. George Gross is a co-founder of POWERWORLD and served on its Board of Directors from 1996–2001. Dr. Gross won the Franz Edelman Management Science Achievement Award in 1985 and is the recipient of several prize paper awards from IEEE and HICSS.

Prof. Gross has consulted on electricity issues with utilities, government organizations and research institutions in North America, Europe, South America, Australia and Asia. He has lectured widely and has given numerous invited presentations at leading universities and research institutions throughout the world. His numerous publications have appeared in the leading journals in the field and his research results have been presented at a wide array of international conferences. He has made a broad range of contributions in various areas of power system planning, operations, analysis and control. His work on smart grid issues has focused on both the technical and the regulatory aspects. The principal areas of involvement include the design of AMI architectures to ensure cyber security, the deployment of AMR for demand response, the integration of demand response, renewable and storage resources into the grid and the economics of smart grid implementation.